Biodistribution and clearance of quantum dots in small animals

Yana F. Salykina*[1], Victoria V. Zherdeva[1], Sergey V. Dezhurov[2], Maxim S. Wakstein[2], Marina.V. Shirmanova[3], Elena.V. Zagaynova[3], Andrey A. Martyanov[4], Alexander P. Savitsky[1]

[1] A.N. Bakh Biochemistry Institute of RAS, [2] Applied Acoustics Research Institute, Center of High Technologies, [3] Nizhny Novgorod State Medical Academy, [4]Lomonosov Moscow State University

*salykina_yana@mail.ru

ABSTRACT

CdSe-core, ZnS-capped semiconductor nanoparticles - quantum dots (QDs) - have been at the forefront of biomedical nanotechnology research thanks to their unique optical и photophysical properties. In the present study the impact of the particle coating and size on their *in vivo* fate after intravenous (IV) injection into mice was studied by fluorescence methods. For this study, we compared organ-selective biodistribution and elimination routes of synthesized QDs coated with 3-mercaptopropionic acid (QD MPA) and commercially available Qtracker 705 nontargeted quantum dots with poly(ethylene glycol) coating (QD PEG). We observed primary accumulation of these QDs in lung. Experiments demonstrated that QD MPA and QD PEG have both remained fluorescent in lung after at least 24 hours postinjection. Moreover, QDs was seen to deposit mainly in liver, spleen, kidney and lymph nodes. We also concluded that QDs MPA and QDs 705 are both sequestered and not excreted with feces or urine.

Keywords: quantum dots, fluorescence, biodistribution, excretion, bioimaging, laser spectrometry, mice.

1. INTRODUCTION

Recent breakthroughs in biomedical nanotechnology have demonstrated the promising clinical applicability of nanostructures. Of the existing biomedically applied nanotechnologies to date, CdSe-core, ZnS-capped semiconductor nanocrystals (also known as quantum dots, QDs) have been at the forefront of biomedical nanotechnology research thanks to their unique optical и photophysical properties [1, 2]. They emit different wavelengths over a broad range of the light spectrum from visible to infrared, depending on their size and chemical composition [3, 4], in addition to single-wavelength excitation. Colloidal quantum dots are bright, photostable fluorophores of a few nanometers in diameter [5]. In addition, quantum dots are more photostable than the best organic fluorophores [6]. Solubilisation of QDs is essential for many biological applications. To render them biologically compatible/active, newly synthesized QDs are "functionalized," or given secondary coatings, which improves water solubility, QD core durability, and suspension characteristics and assigns a desired bioactivity [7].

The many potential biomedical applications of QDs have been recently and extensively reviewed elsewhere [8, 9]. The narrow emission and broad absorption spectra of QDs makes them well suited to multiplexed imaging. QDs are being explored for use in whole-body *in vivo* imaging of normal and tumor tissues, in multicolor *in vitro* fluorescent labelling of cell surface molecules and cellular proteins. QDs may also find use for many other purposes *in vivo*, for example, as long-circulating vascular markers [10, 11], for mapping the reticuloendothelial system [12], for lymph node mapping [13], for detection of cancer cells. Bioconjugated QDs are also being explored as targeted diagnostic cancer-imaging agents and drug-delivery systems [1].

Despite the immense potential for the medical applications of QDs, we know little about the metabolism and health consequences of QDs in organism. Progress is currently impeded by a lack of understanding of how nanostructures interact with biological systems. It is not known, what long-term consequences for an organism accumulation of toxic components of a core of nanoparticles (cadmium, selenium, etc.) will result despite an inert, nontoxic multilayered shell [14, 15]. Many *in vitro* studies have suggested that nanomaterials induce toxic responses through mechanisms such as particle breakdown and the subsequent release of toxic metals [16]. Recently, some studies have investigated the *in vivo*

biodistribution of QDs [17-20]. All of the reports in the literature were unanimous in concluding that QDs show a preference for deposition in organs and tissues and that they do not remain circulating in the bloodstream [21]. Kim et al. demonstrated that from the real-time imaging of live animals treated with the hyaluronic acid (HA)-conjugated QDs, the luminescence of NIR QDs could be detected for up to 2 months [22]. Ballou et al. reported that QDs coated using an amphiphilic poly(acrylic acid) polymer remain fluorescent after at least four months *in vivo* [23].

Potential toxicity of QDs *in vivo* is expected to be determined by many parameters including dose, route of exposure, absorption, distribution in organism, metabolism and excretion. In addition, nanoparticle surface chemistry, chemical composition, size, shape and aggregation have been shown to influence toxicity of nanomaterials. In the present study the impact of the particle coating and size on their *in vivo* fate after intravenous (IV) injection into nude and CD-1 mice was studied by fluorescence methods. For this study, we compared organ-selective biodistribution and elimination routes of synthesized QDs coated with 3-mercaptopropionic acid (QDs MPA) and commercially available Qtracker 705 nontargeted quantum dots with poly(ethylene glycol) coating (QDs 705). QDs localization was monitored by fluorescence whole body imaging, by fluorescent laser spectrometry and confocal fluorescent microscopy of tissue samples.

2. MATERIALS AND METHODS

2.1. Quantum dots

2.1.1. Synthesis and characterization of water soluble CdSe/CdS/ZnSMPA QDs

Instruments and materials

Oleic acid (OA) 99%, cadmium oxide 99.99% were purchased from Alfa, cadmium acetate 99.9%, 1-octadecene (ODE) 90%, oleylamine (OLA) 70%, zinc acetate 99.99%, sulfur 99.99%, tetramethylammonium hydroxide pentahydrate 97% were purchased from Aldrich. Trioctylphosphine (TOP) 99%, trioctylphosphine oxide (TOPO) 90%, hexadecylamine (HDA) 99%, 3-mercaptopropionic acid (MPA) 99% (Fluka), selenium 99.9% (Merck), 1-butanol 99.8%, methanol 99%, rhodamine 6G 99% were purchased from Acros. Chloroform, hexane, toluene, NaOH, Na_2HPO_4, phosphoric acid were chemically pure. PES syringe filters 0.22 μm; PD-10 columns were purchased from GE Healthcare. Fluorescence measurements were carried out using spectrofluorometer Cary Eclipse (Varian). Absorption spectra were recorded using spectrophotometer Cary 100 (Varian). Determination of hydrodynamic size of particles was performed using Nanotrac Ultra (Microtrac).

Hydrophobic CdSe/CdS/CdZnS/ZnS QDs were synthesized in accordance with an earlier protocol [24] with some modifications.

Synthesis of CdSe core nanocrystals. Cadmium acetate 0.401 mmol, OLA 6.08 mmol, TOPO 10.4 mmol, HDA 8.28 mmol and TOP 2.00 ml were added into a 50 mL three-necked flask and were kept in vacuo for one hour at 100°C. The mixture was then heated to 360°C and cooled to 300-260C (depending on the required size of the QDs) under Ar flow. After that 2 mL of 2 M TOPSe solution was quickly injected with a syringe. The reaction was stopped after 10 - 300 seconds by the injection of cooled hexane (10 mL). The reaction mixture was diluted with 10 mL of toluene and 10 mL of butanol. The nanocrystals were precipitated with methanol until the solution became visually turbid. The mixture was centrifuged until the particles were fully precipitated. The precipitate was redispersed in 6 mL of hexane:butanol:toluene mixture (1:1:1) and was reprecipitated with methanol as described above. The precipitation procedure was repeated 3 times. The obtained precipitate of CdSe QDs was dissolved in 5 mL of hexane and centrifuged in order to remove aggregates. The concentration of the obtained particles was estimated spectrophotometrically [26].

Synthesis of CdSe/CdS/CdZnS/ZnS core/shell/shell nanocrystals. The CdSe QDs solution (~ 0.1 μmol) was injected into the mixture of 2 g ODA and 6g ODE at 230°C under Ar and stirred. For covering CdSe cores quantity of the Zn, Cd and S precursors was calculated as described elsewhere [24]. Corresponding metal and halcogenide precursors were 0.2 M of zinc acetate in ODE:OLA 3:1, 0.2 M cadmium oleate in ODE and 0.2 M sulfur in ODE respectively. Covering procedure was analogous to the above-mentioned paper [24], using 3-4 monolayers of CdS, 3-4 monolayers of CdZnS and 4-5 monolayers of ZnS on the demanded emission wavelength. Synthesized QDs were isolated from the reaction

mixture in the same way as the CdSe core nanocrystals. Finally, nanocrystals were dissolved in $CHCl_3$ to a concentration of 10 μM.

Surface modification with MPA. Hydrophilization was performed as described elsewhere [25]. The10 μM solution of hydrophobic QDs in $CHCl_3$ was cooled under Ar to 0°C. The mixture of solutions of tetramethylammonium hydroxide pentahydrate (1M) and MPA (1 M) in $CHCl_3$ was injected via septum to a final concentration of MPA 0.13 M. The mixture was stirred at this temperature for one hour. Then the QDs were precipitated with NH_3 saturated methanol (1:1 v/v). The precipitate was isolated by centrifugation, washed with diethyl ether and dried under vacuum. After that the QDs were dispersed in 25 mM phosphate buffer. A small amount of aggregates (less than 5 weight %) were removed by centrifugation and filtration through the 0.22 μm membrane filter.

The concentration of the QDs was estimated spectrophotometrically [26]. The fluorescence quantum yield of the QDs was determined using a previously described relative optical method [27] Rhodamine 6G (with ethanol as the solvent) was chosen as a reference standard (QY 95%). Synthesized QDs MPA had the quantum yield in the range of 10-40 %. QDs MPA exhibit an emission wavelength of about 620 and 630 nm. Variation of fluorescence emission peaks of the QDs samples associated with slight differences in particle sizes produced during the synthesis. Measurements of the hydrodynamic diameters were performed using dynamic light scattering (DLS) on Nanotrac Ultra (Microtrac). For measurements, pH of the aqueous solution of QDs was set to be 8.0 using 25 mM phosphate buffer. We performed four measurements with acquisition time 60 s. The average size of the QDs MPA was estimated to be ~ 8 – 11 nm.

2.1.2. QDs 705

Commercial Qtrackers 705 nontargeted quantum dots with an emission maximum around 700-715 nm are purchased from Invitrogen. Each particle has a CdTe/ZnS QDs with a core diameter of ~10-15 nm. Qtrackers 705 nontargeted QDs are described by the manufacturer as having a poly(ethylene glycol) PEG surface coating specially developed to minimize nonspecific interaction and to reduce immune response by the tissues [23]. Each tube of this product contained 200 μL of a 2μM solution in 50 mM borate buffer, pH 8.3.

2.2. Animals

Female nude and CD-1 mice were obtained from farm of laboratory animals “Pushino” of M.Shemyakin and Yu. Ovchinnikov Institute of Bioorganic Chemistry of Russian Academy of Sciences, Russia. All animals acclimated to the animal facility for at least 48 h prior to experimentation. Mice were kept in a barrier under HEPA filtration and in a 12h/12h light/dark cycle, and given food and water ad libitum. They were at 12 weeks of age and weighed 20 to 25 g at time of QDs injection.

For mouse injection, the solutions of QDs were prepared in sterile 1xPBS buffer or 20 mM phosphate buffer. To characterize the biodistribution and accumulation of the QDs, the intravenous dose (290 pmol QDs MPA and 40 pmol QDs 705 per animal) was given as a bolus in a volume of 0.1 mL into the jugular vein (n=3 for each time point, and each QDs type) of nude or CD-1 mice.

The mice were anesthesized by Zoletil (20 mg/ml, 50 μl per animal) and Rometar 2% (10 μl per animal) intramuscularly for *in vivo* imaging and prior to sacrifice. The mice were sacrificed by cervical dislocation 20 min, 40 min, 1.5 h, 4 h, 24 h и 48 h after injection of QDs and tissue specimens from the lung, heart, liver, kidneys, spleen, brain, intestine (section 10 mm in length), stomach, muscle, bladder and lymph nodes were removed, washed in PBS buffer and taken for analysis by fluorescent laser spectrometry and confocal fluorescent microscopy. For control measurements tissue specimens were taken from the same kind of organs of mice which were kept in the same conditions as experimental mice but not administered QDs.

All experimental procedures were approved by the local ethical committee for animal experiments. Animals were treated humanely with regard for alleviation of suffering.

2.3. Fluorescent imaging

Whole body images were acquired on the imaging system iBox (UVP, USA) equipped a darkroom box, a motorized five-position emission filter wheel, an overhead lighting (UV (365 nm), Visi-blue™ (480 nm) and white light) and power lift. The filtered fluorescence signal is measured by a high sensitivity, 16-bit monochrome cooled CCD camera (BioChemi HR Camera, UVP, USA) with resolution 2048x2048, placed in the top of darkroom. Animals were illuminated using a 150-Watt quartz halogen automated multispectral light sourse BioLite (UVP, USA) designed for use with ferrule fiber optics bundles. The integrate excitation filter wheel accommodates up to 8 filters. Image processing is controlled by the Vision WorksLS software (UVP, USA).

Excitation filters were 502-547 nm, emission filters were 605-680 nm for QDs MPA and 665-720 for QDs 705. Imaging times varied with time postinjection and were adjusted to give maximum dynamic range (over a 48 h period); time of exposition of 25 s was normally used.

2.4. Fluorescent laser spectrometry

For *ex vivo* investigation, major organs were harvested and subjected to analysis by the method of fluorescent laser spectrometry using multispectral fluorescent system Spectrum-Cluster (Institute of General Physics of RAS) with laser excitation source. The system is equipped by the fiber-optical laser composed of seven fibers (d 100 μm) with a numerical aperture of 0.22 for the fluorescence registration and single fiber (d 110 μm) for fluorescence excitation. The system uses three continuous laser light sources with an excitation wavelength in the visible spectrum range. Spectral range of emission depends on the excitation source (410-900 nm). An Nd^{3+}: YAG diode-pumped laser, the wavelength of which is 532 nm and power - 10 mW, was used for this experiment. Identification of the QDs was carried out by the presence of characteristic peaks in fluorescence spectra of tissue samples *ex vivo*.

2.5. Confocal fluorescent microscopy

Biodistribution and accumulation of the QDs after intravenous injection were analyzed by the method of confocal fluorescent microscopy using a system for a confocal laser scanning and multiphoton microscopy Axiovert 200M LSM 510 META (Carl Zeiss, Germany) equipped with an inverted Carl Zeiss Axiovert 200 MOT microscope. All images were performed using spectral module Carl Zeiss 23 META for detecting of backscattered light in a range of 400-700 nanometers with the permission of 10 nm.

Collecting samples of organs and tissues was produced 40 min after injection of quantum dots. Tissue specimens taken from the organs (the size of 3-4 mm) were placed on the microscope stage for the analysis of fluorescence. Confocal images were obtained in reflected light and in fluorescence mode. To identify the fluorescence of QDs spectral data were recorded. Fluorescent and pseudo-color spectral images were obtained using one-photon excitation at a wavelength of 488 nm. Emission filters were in the range of 650-710 nm for fluorescence and 512-704 nm for the pseudo-color spectral images. Size of images was 225x225 μm.

2.6. Excretion studies

To address further whether the QDs were eliminated into urine or feces, mice (n=3) were given jugular-vein injections of QDs MPA (290 pmol in a volume of 0.1 mL), QD705 (40 pmol in a volume of 0.1 mL), or saline (control) and were kept in Techniplast (Italy) metabolic cages. Each animal was housed in a collection cage for 72 h; urine and feces probes were collected daily and analyzed by the method of fluorescent laser spectrometry using multispectral fluorescent system Spectrum-Cluster (IGP, RAS).

3. RESULTS AND DISCUSSION

In the first set of experiments dynamic biodistribution of synthesized 620 nm-emitting QDs coated with 3-mercaptopropionic acid (QDs MPA) after injection into the jugular vein of mice was studied using the bioimaging automated system iBox (UVP, USA). Images were obtained for control animal group and at various time points after injection (up to 48 h). This studying has shown primary accumulation of QDs in lung and some departments of heart, in particular in the left and right atrium (Figure 1).

The autofluorescence of the gastrointestinal tract upon excitation in the wavelength range 502-547 nm was observed in all animals, including those in the control group, which may be explained by a diet of laboratory mice, probably as well as fluorescence of bile pigments. The most intense fluorescence was detected in the gall bladder, stomach, intestines.
In the second set of experiments the accumulation of QDs MPA in the lung and heart after injection into the jugular vein of nude mice was confirmed by analysis of the fluorescence of organs *ex vivo* using a laser spectrometer Spectrum-Cluster. Fluorescence spectra of specimens taken from these organs 20 min, 40 min, 1.5 h, 4 h, 24 h and 48 h postinjection were measured. A well detectable characteristic fluorescence maximum of QDs MPA at a wavelength of 620 nm was revealed over a 48 h period in the spectra of lung (Figure 2). In the spectra of heart measured over a 24 h period postinjection the presence QDs MPA was also clearly seen, but after 48 h QDs were no longer present in the heart. Different departments of heart were noticed to have different levels of fluorescence intensity with a maximum level in the left atriums.

The method of fluorescence spectroscopy in comparison with planar bioimaging has greater sensitivity, thus it was possible to detect the presence of quantum dots in other vital organs (Figure 3A). High fluorescence signal was obtained for the liver and remained unchanged up to 4 h postinjection; spleen and kidney signals were observed to have lower intensity at the same time period. Further quantification of the fluorescence in the organs after sacrifice 24 h postinjection in comparison to a non-injected control mice shows significant differences in the fluorescence signals only in liver and lung. It can be seen from Figure 3A that there is a significant reduction in the fluorescence in the organs at 48 h postinjection. After 48 h fluorescence of liver was only detected, fluorescence intensity level of other organs was similar to the level of autofluorescence. The distribution pattern of all animals in experimental group was similar.
Daou et al. hypothesized that the substantial loss of fluorescence could be due to either the clearance of the particles from the body (hypothesis 1) or to the loss of their fluorescence signal, which could be due to the slow degradation of the QD core (hypothesis 2) or to a change in their chemical coating (hypothesis 3) [28].

QDs 705 were injected into the jugular vein of CD-1 mice at a low dose (40 pmol per animal). Nevertheless as seen in Figure 3B the dominant signal 20 min after injection was also found in the lung and remained well detectable up to 24 h. Other organs with readily detectable QDs distribution included the heart, kidney and spleen, but their signal intensity was very low. Those findings partially contradict earlier present data. Yang et al. assessed the tissue disposition and pharmacokinetics of commercially available Qtracker 705 nontargeted QDs in mice. The authors demonstrated that 44 to 50% of tail-vein injected QDs 705 retained in carcass (muscle, skin, bone). In addition, tissue localization of QDs 705 were mainly in liver, kidney and spleen, but not lung (not more than 0,5% of the injected dose). Lin et al. performed in-depth pharmacokinetic and toxicology studies of QDs 705 in mice at time points of up to 6 months. According to their results, these QDs injected intravenously into tail vein of mice accumulated primarily within the liver, spleen, and kidney [29]. Probably, the difference in results can be explained by the hypothesis that an injection site (tail or jugular vein) can influence the distribution and accumulation of QDs.

However, our experiments demonstrated that QD MPA and QD PEG have both remained fluorescent in lung after at least 24 hours postinjection. This trapping of QDs in the 'lung barrier' may be associated with multifocal organizing thrombi in the pulmonary arteries, following a local injection of high concentrations of samples. Geys et al. investigated the inflammatory properties and prothrombotic effects of QDs with carboxyl and amine surface coatings after intravenous injection [30]. They have shown that at high doses (3,600 and 720 pmol/mouse), QDs caused pulmonary vascular thrombosis, most likely by activating the coagulation cascade via contact activation, with carboxyl-QDs being more potent in inducing this effect than amine-QDs. In tissue distribution studies, QDs were found mainly in the lung and liver. Ramot et. al. reported histopathological evidence for prothrombotic adverse effects mediated by QDs labeling [31]. They demonstrated that non-QDs labeled human embryonic palatal mesenchymal (QD-HEPM) cells did not lead to thrombi in the lung vessels, whereas the administration of a single IV injection of QD-HEPM cells to male NOD/SCID mice was found to be associated with minimal to mild, multifocal organizing thrombi in the pulmonary arteries of all treated animals at one week postinjection. Interestingly, these thrombi underwent spontaneous regression. This observation is in agreement with our results, where gradual decrease of fluorescence intensity in the lung was observed.

The sensitivity of the spectral methods used in our work is limited by the studying of the subsurface fluorescence, so the biodistribution of 630 nm-emitting QDs MPA in an organism of animals after intravenous injection proved to be true at research of organs' and tissues' samples by the methods of confocal fluorescent microscopy. For this purpose animals were anesthetized in lethal doses on the 40-th min - in a point of maximum accumulation QDs, their major organs (a skin, muscles, a brain, lung, a liver, a spleen, kidneys, heart, a small intestines, lymph nodes) surgically exposed and

imaged using a system for a confocal laser scanning and multiphoton microscopy Axiovert 200M LSM 510 META (Carl Zeiss, Germany). QDs MPA were found by the method of confocal fluorescent microscopy mainly in lung, liver, spleen, kidney and lymph nodes (in decreasing order of fluorescence). Microscopy confirmed the presence of characteristic peaks of the QDs at a wavelength of 630 nm (data not shown). Nanoparticles were distributed mainly in the intercellular space in the liver and presumably in the cytoplasm of cells in the spleen. Moreover, QDs was seen to deposit in sites of blood supply of the heart, skin, and muscles as well as of the brain. It is worth noting that there are no reports to date describing the migration of injected QDs into the brain. Whether this means that QDs are incapable of crossing the blood-brain barrier or whether they are simply cleared too quickly from the blood circulation by cells of the reticuloendothelial system is a question which has not yet been assessed [21]. Probably, localization of QDs in the lung, liver, spleen and lymph nodes indicates that the nanoparticles are absorbed as foreign agents by mononuclear phagocytes, which may be involved in the utilization of QDs. Fischer et al. have shown that mercaptoundecanoic acid-coated and lysine-crosslinked QDs were predominantly sequestered by the liver, with notable uptake also occurring in the spleen, kidneys, and bone marrow (organs that are part of the reticuloendothelial system, RES) [17]. The electron microscopy images showed that QDs were trapped in vesicles in Kupffer cells of the liver and that the QDs appeared to enter the cells via phagocytic processes. Gao et al. reported the relatively high accumulation of near-infrared InAs/InP/ZnSe QDs coated by mercaptopropionic acid (MPA) in the RES system (e.g., liver and spleen), whereas human serum albumin (HSA)-coated QDs-MPA showed reduced localization in mononuclear phagocytic system-related organs due to the low uptake of these QDs in macrophage cells [32]. These findings allowed to conclude that because of the negative surface charge the QDs-MPA may physically absorb the proteins in the blood vessels and tend to be recognized and engulfed by the macrophage cells.

Finally, feces and urine were collected over a 72 h period after injection of 620 nm-emitting QDs MPA into the jugular vein of nude mice and analyzed by method of fluorescent laser spectrometry to determine if the QDs were cleared via the bile, intestinal lumen, or kidney. Fluorescence of feces samples measured using the laser spectrometer was not significantly different from background values of control mice (Figure 4A). In the spectra of urine samples a peak at 610 nm appeared (Figure 4B). Normalizing of the received spectra on the maximum intensity of fluorescence has shown, that this peak have also been present in the control sample of urine, therefore does not concern fluorescence of QDs (data no shown). It is worth to note that general fluorescence intensity of urine samples gradually increased for up to 72 h postinjection, that, probably, may be explained accumulation of any fluorescent metabolits and demands additional studying. Probes of urine and feces were also taken after administration of QDs 705 into the jugular vein of CD-1 mice, but no traces of these QDs were detected in any probe. Previously, Yang et al., and then Lin et al. reported similar results. The authors could find no evidence of excretion or metabolism of the QD705 nanoparticles within 28 days following dosing [20, 29]. Finally, we therefore concluded that QDs MPA and QDs 705 are both sequestered and not excreted.

To date, there have been a few studies in the literature which have looked at the excretion of QDs following their in vivo administration. Fischer et al. [17] reported that mercaptoundecanoic acid-coated and lysine-crosslinked QDs not detected in feces or urine for up to ten days after intravenous dosing in Sprague-Dawley rats. In contrast to the results described above, other studies have demonstrated efficient excretion of QDs by mice. For example, Choi et al. demonstrated that, coated with cysteine CdSe/ZnS QDs with a zwitterionic charge and hydrodynamic diameter (HD) less than approximately 5.5 nm are effectively cleared from the body through urine and bile. In this study, the authors employed fluorescent QDs as a model system to define the HD and surface charge combination that permits rapid body elimination of nanometer-sized objects [19]. According to observation of Choi et al. the absence of renal clearance of QDs MPA and QDs 705 in our study can be explained by the large HD ($\geq$ 10 nm) or anionic surface charge of these QDs .

4. CONCLUSION

We have estimated the *in vivo* pharmacokinetics of synthesized QDs coated with 3-mercaptopropionic acid (QD MPA) and commercially available Qtracker 705 nontargeted quantum dots with PEG coating and their uptake by various organs after injection into jugular vein of mice. The results show elective accumulation of both QDs in certain organs and tissues at hit in a blood-groove. We observed primary accumulation of QDs MPA in lungs and atriums of heart, and QDs 705 in lungs. Experiments demonstrated that QD MPA and QD PEG have both remained fluorescence in lungs after at least 24 hours postinjection. Moreover, QDs MPA was seen to deposit mainly in liver, spleen, kidney and lymph nodes

(in decreasing order of fluorescence), and in sites of blood supply of the skin, and muscles as well as of the brain. Finally, we therefore concluded that QDs MPA and QDs 705 are both sequestered and not excreted with feces or urine.

5. ACKNOWLEDGEMENTS

This study was supported by grants No. 01.648.11.3003 and No. 01.648.11.3006 from the Federal Agency for Science and Innovation.

This work was partially supported by grant No. 09-04-12263 from the RFBR.

6. REFERENCES

1. Medintz, I. L., Uyeda, H. T., Goldman, E. R., and Mattoussi, H. , "Quantum dot bioconjugates for imaging, labelling and sensing," Nat Mater 4(6), 435-446 (2005).
2. Klostranec, J.M. and W.C.W. Chan, "Quantum Dots in Biological and Biomedical Research: Recent Progress and Present Challenges" Advanced Materials 18(15, 1953-1964 (2006).
3. Bailey, R.E. and S. Nie, "Alloyed semiconductor quantum dots: tuning the optical properties without changing the particle size" J Am Chem Soc 125(23), 7100-7106 (2003).
4. Qu, L. and X. Peng, "Control of photoluminescence properties of CdSe nanocrystals in growth", J Am Chem Soc 124(9), 2049-2055, (2002).
5. Ghasemi, Y., P. Peymani, and S. Afifi, "Quantum dot: magic nanoparticle for imaging, detection and targeting", Acta Biomed 80(2), 156-165, (2009).
6. Resch-Genger, U., Grabolle, M., Cavaliere-Jaricot, S., Nitschke, R., and Nann, T., "Quantum dots versus organic dyes as fluorescent labels", Nat Methods 5(9), 763-775, (2008).
7. Mazumder, S., Dey, R., Mitra, M. K., Mukherjee, S., and Das, G. C., "Review: Biofunctionalized Quantum Dots in Biology and Medicine", Journal of Nanomaterials 2009, 1-18, (2009).
8. Jamieson, T., Bakhshi, R., Petrova, D., Pocock, R., Imani, M., and Seifalian, A. M., "Biological applications of quantum dots. Biomaterials", 28(31), 4717-4732, (2007).
9. Azzazy, H.M., M.M. Mansour, and S.C. Kazmierczak, "From diagnostics to therapy: prospects of quantum dots. Clin Biochem", 40(13-14), 917-927, (2007).
10. Lim, Y. T., Kim, S., Nakayama, A., Stott, N. E., Bawendi, M. G., and Frangioni, J. V., "Selection of quantum dot wavelengths for biomedical assays and imaging", Mol Imaging 2(1), 50-64, (2003).
11. Smith, J. D., Fisher, G. W., Waggoner, A. S., and Campbell, P. G., "The use of quantum dots for analysis of chick CAM vasculature",. Microvasc Res 73(2), 75-83, (2007).
12. Hanaki, K., Momo, A., Oku, T., Komoto, A., Maenosono, S., Yamaguchi, Y., and Yamamoto, K., "Semiconductor quantum dot/albumin complex is a long-life and highly photostable endosome marker", Biochem Biophys Res Commun 302(3), 496-501, (2003)
13. Kim, S., Lim, Y. T., Soltesz, E. G., De Grand, A. M., Lee, J., Nakayama, A., Parker, J. A., Mihaljevic, T., Laurence, R. G., Dor, D. M., Cohn, L. H., Bawendi, M. G., and Frangioni, J. V., "Near-infrared fluorescent type II quantum dots for sentinel lymph node mapping", Nat Biotechnol 22(1), 93-97, (2004).
14. Bertin, G. and D. Averbeck, "Cadmium: cellular effects, modifications of biomolecules, modulation of DNA repair and genotoxic consequences (a review)", Biochimie 88(11), 1549-1559, (2006).
15. Vinceti, M., Wei, E. T., Malagoli, C., Bergomi, M., and Vivoli, G., "Adverse health effects of selenium in humans", Rev Environ Health 16(4), 233-251, (2001).
16. Hardman, R., "A toxicologic review of quantum dots: toxicity depends on physicochemical and environmental factors", Environ Health Perspect 114(2), 165-172, (2006).
17. Fischer, H. C., Liu, L., Pang, K. S., and Chan, W. C. W., "Pharmacokinetics of Nanoscale Quantum Dots: In Vivo Distribution, Sequestration, and Clearance in the Rat", Advanced Functional Materials 16(10), 1299-1305, (2006).
18. Gopee, N. V., Roberts, D. W., Webb, P., Cozart, C. R., Siitonen, P. H., Warbritton, A. R., Yu, W. W., Colvin, V. L., Walker, N. J., and Howard, P. C., "Migration of intradermally injected quantum dots to sentinel organs in mice", Toxicol Sci 98(1), 249-257, (2007).
19. Choi, H. S., Liu, W., Misra, P., Tanaka, E., Zimmer, J. P., Itty Ipe, B., Bawendi, M. G., and Frangioni, J. V., "Renal clearance of quantum dots", Nat Biotechnol 25(10), 1165-1170, (2007).

20. Yang, R. S., Chang, L. W., Wu, J. P., Tsai, M. H., Wang, H. J., Kuo, Y. C., Yeh, T. K., Yang, C. S., and Lin, P., "Persistent tissue kinetics and redistribution of nanoparticles, quantum dot 705, in mice: ICP-MS quantitative assessment", Environ Health Perspect 115(9), 1339-1343, (2007).
21. Pelley, J.L., A.S. Daar, and M.A. Saner, "State of academic knowledge on toxicity and biological fate of quantum dots", Toxicol Sci 112(2), 276-296, (2009).
22. Kim, J., Kim, K. S., Jiang, G., Kang, H., Kim, S., Kim, B.-S., Park, M. H., and Hahn, S. K., "In vivo real-time bioimaging of hyaluronic acid derivatives using quantum dots", Biopolymers, 89(12), 1144-1153, (2008).
23. Ballou, B., Lagerholm, B. C., Ernst, L. A., Bruchez, M. P., and Waggoner, A. S., "Noninvasive imaging of quantum dots in mice", Bioconjug Chem 15(1), 79-86, (2004).
24. Xie, R., Kolb, U., Li, J., Basche, T., and Mews, A., "Synthesis and characterization of highly luminescent CdSe-core CdS/Zn0.5Cd0.5S/ZnS multishell nanocrystals", J Am Chem Soc 127(20), 7480-7488, (2005).
25. Pong, B.K., B.L. Trout, and J.Y. Lee, "Modified ligand-exchange for efficient solubilization of CdSe/ZnS quantum dots in water: a procedure guided by computational studies", Langmuir 24(10), 5270-5276, (2008).
26. Yu, W. W., Qu, L., Guo, W., and Peng, X., "Experimental determination of the extinction coefficient of CdTe, CdSe, and CdS nanocrystals", Chem. Mater 15, 2854-2860, (2003).
27. Grabolle, M., Spieles, M., Lesnyak, V., Gaponik, N., Eychmuller, A., and Resch-Genger, U., "Determination of the fluorescence quantum yield of quantum dots: suitable procedures and achievable uncertainties", Anal. Chem 81, 6285–6294, (2009).
28. Daou, T. J., Li, L., Reiss, P., Josserand, V., and Texier, I., "Effect of poly(ethylene glycol) length on the in vivo behavior of coated quantum dots", Langmuir 25(5), 3040-3044, (2009).
29. Lin, P., Chen, J. W., Chang, L. W., Wu, J. P., Redding, L., Chang, H., Yeh, T. K., Yang, C. S., Tsai, M. H., Wang, H. J., Kuo, Y. C., and Yang, R. S., "Computational and ultrastructural toxicology of a nanoparticle, Quantum Dot 705, in mice", Environ Sci Technol 42(16), 6264-6270, (2008).
30. Geys, J., Nemmar, A., Verbeken, E., Smolders, E., Ratoi, M., Hoylaerts, M. F., Nemery, B., and Hoet, P. H., "Acute toxicity and prothrombotic effects of quantum dots: impact of surface charge", Environ Health Perspect 116(12), 1607-1613, (2008)
31. Ramot, Y., Steiner, M., Morad, V., Leibovitch, S., Amouyal, N., Cesta, M. F., and Nyska, A., "Pulmonary thrombosis in the mouse following intravenous administration of quantum dot-labeled mesenchymal cells", Nanotoxicology 4(1), 98-105, (2010).
32. Gao, J., Chen, K., Xie, R., Xie, J., Lee, S., Cheng, Z., Peng, X., and Chen, X., "Ultrasmall near-infrared non-cadmium quantum dots for in vivo tumor imaging", Small 6(2), 256-61, (2010).

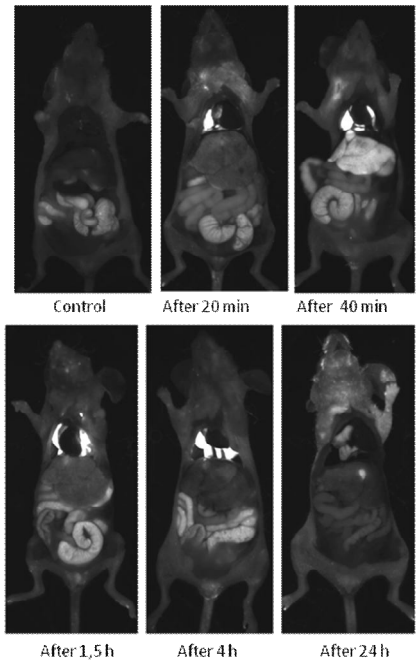

Figure 1. Nude mice imaged at various time points postinjection of 620 nm-emitting QDs MPA into the jugular vein; skin, sternum and peritoneum removed. The images obtained have shown the presence of fluorescent signal in atriums of the heart and lung (in the images - the bright areas of high signal intensity) within 4 hours after injection of QDs. A low fluorescent signal was also observed in lung after 24 h postinjection. Images obtained 48 h postinjection did not differ from control images. The images have been taken using a time of exposition of 25 s, excitation filter 502-547 nm and emission filter 605-680.

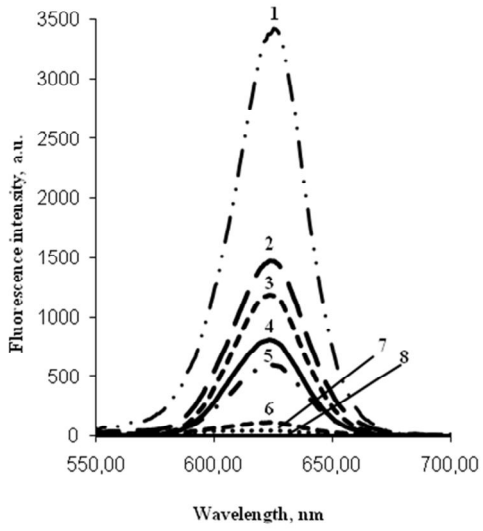

Figure 2. Fluorescence spectra of the lung after injection of 620 nm-emitting QDs MPA into the jugular vein of nude mice. 1 – QDs MPA in buffer; 2 – lung 40 min postinjection; 3 – lung 20 min postinjection; 4 – lung 1,5 h postinjection; 5 – lung 4 h postinjection; 6 – lung 24 h postinjection; 7 – lung 48 h postinjection; 8 – lung control. Excitation wavelength 532 nm.

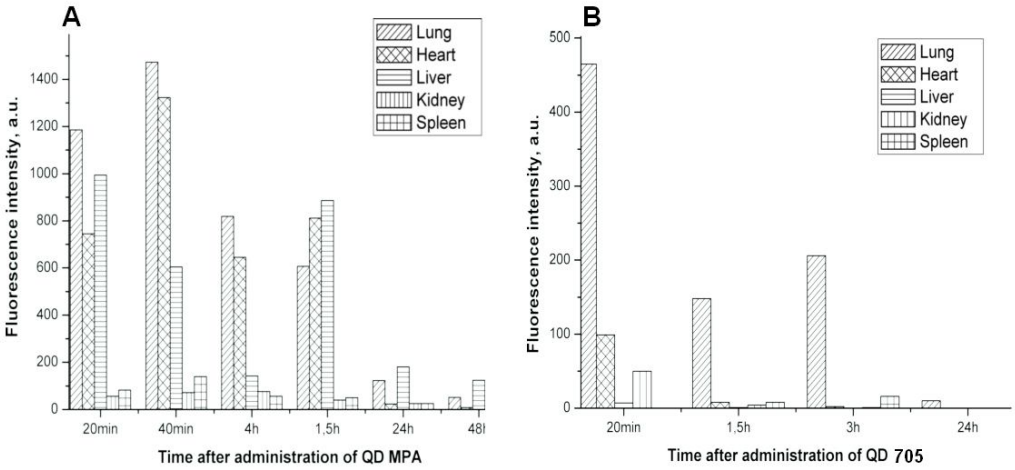

Figure 3. Dynamics of change of a fluorescent signal in lung, heart, liver, spleen and kidney after injection of 620 nm-emitting QDs MPA into the jugular vein of nude mice (A) and QDs 705 into the jugular vein of CD-1 mice (B). A closer comparison showed a greater uptake of QDs MPA than QDs 705 by the lung, heart and liver, suggesting that the uptake was dependent on surface modification. Excitation wavelength 532 nm.

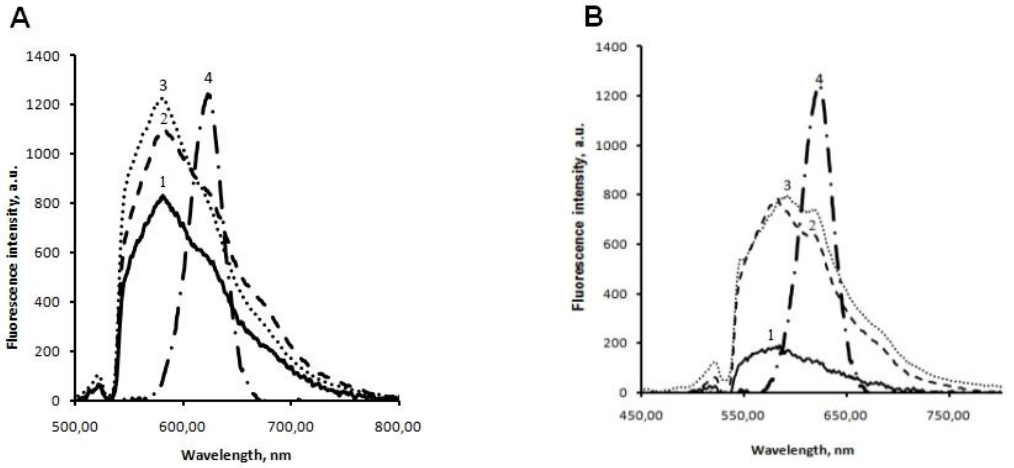

Figure 5. Fluorescence spectra of the feces (A) and urine probes (B) after injection of 620 nm-emitting QDs MPA into the jugular vein of nude mice. Mice were kept in metabolic cages; urine and feces probes were collected daily and analyzed by the method of fluorescent laser spectrometry. Excitation wavelength 532 nm.

(A) 1 – feces control; 2 – feces 24 h postinjection; 3 – feces 48 h postinjection; 4 – QDs MPA in buffer.

(B) 1 – urine control; 2 – urine 24 h postinjection; 3 – urine 48 h postinjection; 4 – QDs MPA in buffer.